Received: 11 September 2025 | Revised: 6 November 2025 | Accepted: 17 December 2025

DOI: 10.1111/jmi.70058

Journal of Microscopy RMS

ORIGINAL ARTICLE

Determining bismuth content in GaAsBi alloys by energy-dispersive X-ray spectroscopy: A case study with multiple sets of *k**-factors for analytical transmission electron microscopy

T. Walther

School of Electrical & Electronic Engineering, University of Sheffield, Sheffield, UK

Correspondence
T. Walther, School of Electrical & Electronic Engineering, University of Sheffield, Mappin Building, Mappin Street, Sheffield S1 3JD, UK.
Email: t.walther@sheffield.ac.uk

Abstract

Measuring the bismuth (Bi) content of ternary gallium arsenide bismuthide (GaAsBi) alloys is important because it sensitively influences their bandgap, and Bi is known to segregate vertically to the surface and sometimes also laterally during growth, so elemental distribution maps need to be quantified. A suitable method is mapping of characteristic X-rays based on energy-dispersive X-ray spectroscopy (EDXS) in a scanning transmission electron microscope (STEM). One of the key problems in this alloy system that there are several overlaps of characteristic X-ray lines from the corresponding elements, namely of As Kα with Bi Lα and of a sum peak of Ga Lα and As Lα with Bi Mα, which no standard solid-state detector could distinguish. Routine quantification procedures thus often fail, exhibiting unacceptably large scatter. Here, an iterative procedure using *k**-factors is outlined, leading to improved quantification using sets of different X-ray line pairs to be consistent within better than 1% bismuth coverage of the group V sub-lattice, for a range up to 14%.

KEYWORDS

energy-dispersive X-ray spectroscopy (EDXS), GaAsBi, peak overlaps, scanning transmission electron microscopy (STEM), self-consistent *k*-factors, sum peaks

1 | INTRODUCTION

Bismuth (Bi) was originally used as a surfactant for the growth of gallium arsenide (GaAs) by liquid phase epitaxy in which it was not active as a dopant.[1] GaAsBi, also denoted as Ga(As,Bi) or Ga($As_{1-x}Bi_x$), describes an alloy where heavy Bi atoms replace some fraction x of arsenic (As) atoms in the sphalerite lattice of the compound semiconductor GaAs. The resulting alloy has an increased lattice constant (at only slightly increased density) and a much smaller, direct bandgap that depends sensitively on bismuth content x but relatively little on temperature and so makes this an attractive material for deep infrared (IR) emitters and detectors with little temperature drift. Since 2003 molecular beam epitaxy has been used to grow such layers epitaxially, initially with only

small values of x (maximum of 0.031[2] to 0.045[3]), later with increasing concentrations up to $x = 0.22$ at growth temperatures as lows as 200°C,[4] however, at higher bismuth content Bi segregation can lead to the formation of Bi-rich clusters.[5] A key problem is that photoluminescence spectra and X-ray diffraction patterns of $GaAs_{1-x}Bi_x$ layers are often rather broad, and their simulation depends on assumptions about their lattice parameters, strain relaxation as well as bismuth content, which themselves can only be linked via density functional theory (DFT). DFT, however, lacks reliable materials data partly because a pure GaBi alloy as a possible end-member for $x = 1$ as reference does not exist.[6] These x values refer to the Bi fraction of the group V sub-lattice. Ga makes up the other group III sub-lattice (i.e. 50 at%), so the Bi content only amounts to $50x$ at%, and measuring it precisely to 0.5 at% (for $\Delta x = 0.01$) or better is a real challenge. Current quantification approaches by STEM-EDXS based on standard k-factors show an unacceptably large scatter, depending on which X-ray lines are chosen for quantification, even if absorption corrections are taken into account. This is elaborated in more detail in Section 3.

2 | MONTE CARLO SIMULATIONS AND THEORY

GaAsBi exhibits a family of nine X-ray lines, six of which (Ga: K, L; As: K, L; Bi: L, M) can be used for microanalysis in (S)TEM. These are listed with the energies of their sub-lines in Table 1. The Bi K-lines are too hard X-rays for any standard energy-dispersive X-ray spectrometer to be analysed, even in a medium voltage transmission electron microscope.

Kα_2 lines are about half as strong as Kα_1 lines (hence greyed out in Table 1), and the Lα1 and Lα_2 lines are usually indistinguishable. This system presents a real challenge for any quantitative energy-dispersive X-ray spectroscopy (EDXS) because of two major issues:

(i) There is significant overlap between the energies of Ga Kβ, As Kα and Bi Lα at about 10 keV (marked in green font in Table 1) so the software used for line identification and curve fitting must work extremely well to distinguish these.
(ii) The Bi Mα energy is almost indistinguishably close (with a weighted difference of $\Delta E < 43$ eV well below the energy resolution of any solid-state X-ray detector and closer to the typical 10 eV channel range) to the sum Ga Lα + As Lα (marked in red font), so sum peaks from the main elements Ga and As must be taken into account at high X-ray count rates, as they will likely occur in Bi-poor GaAsBi.

Employing the six main X-ray lines (Ga: K, L; As: K, L; Bi: L, M) it is possible to measure all together 15 intensity binary ratios.

Three of these would be ratios for identical elements (Ga K/L, As K/L, Bi L/M) and can be used to estimate the specimen thickness from their relative differences in absorption: the harder X-rays are less affected by absorption while the softer X-rays are stronger absorbed, so the latter will drop significantly with an increase in foil thickness, hence K/L and L/M ratios should always increase monotonically with thickness.[9–11] Results from Monte Carlo simulations for a standard Si:Li detector[12] are displayed in Figure 1. All curves start near unity for $t = 0$ and then increase very slightly, faster than linear. Here, we used the standard atomic weights and the lattice parameter estimates from Ref. (2) to check that the density of GaAsBi increases actually only very slightly because the mass increase by substituting 1 As atom by 1 much heavier Bi atom (for $x = 0.25$) increases the unit cell volume almost in the same proportion.

The remaining other 12 intensity ratios of lines from different elements can be evaluated in terms of their so-called k-factors that are usually tabulated for thin foils using weight % instead of atomic % and using either Si K (in mineralogy) or Fe K (in metallurgy) as reference lines.[13] We have extended thin foil k-factors to effective k*-factors by multiplying the thin film k-factors with their corresponding absorption correction factors[14,15] so we can plot their variation $k^*(t)$ with specimen foil thickness t (where $\lim_{t\to 0} k^*_{AB}(t) = k_{AB}$). When plotting them as

TABLE 1 Major X-ray line energies for Ga, As and Bi.

Line	Kα_1	Kα_2	Kβ_1	Lα_1	Lα_2	Lβ_1	Lβ_2	Lγ_1	Mα_1
Transition	KL3	KL2	KM3	L3M5	L3M4	L2M4	L3N5	L2N4	M
Element (Z)									
Ga (31)	9252	9225	10,264	1098	1098	1125			
As (33)	10,543	10,508	11,726	1282	1282	1317			
Bi (83)	77,109	74,816	87,344	10,839	10,731	13,024	12,980	15,248	2423

Note: Rounded in units of eV; K- and L-lines from Ref. (7) and M lines from Ref. (8). Green: line overlaps around 10.5 keV; red: possible sum peaks leading to overlap at around 2.4 keV. In particular, the energies of Ga Lα_1 + As Lβ_1, Ga Lβ_1+ As Lα_1 are almost identical to that of Bi Mα_1.

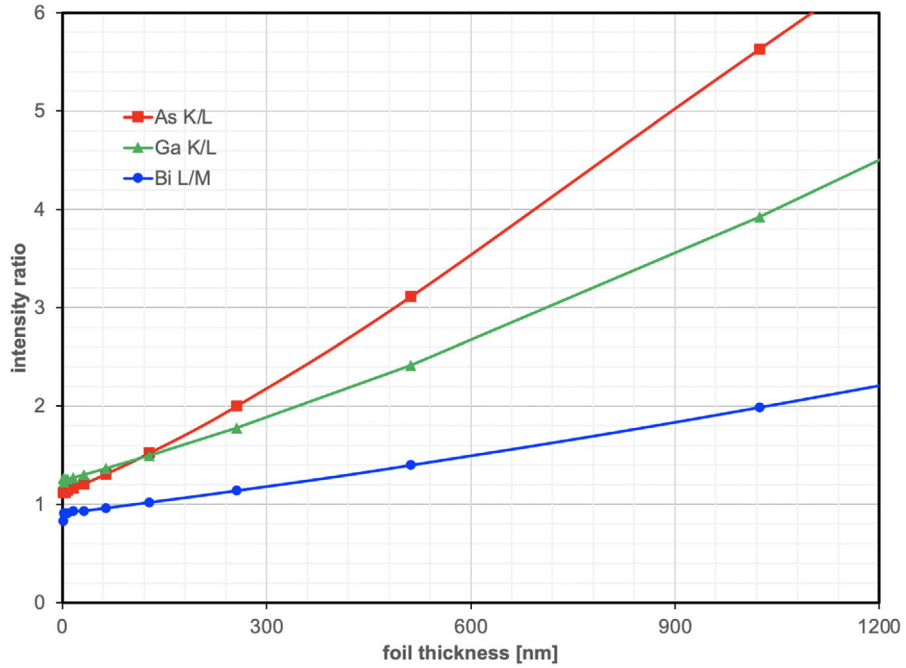

FIGURE 1 Plot of Ga K/L, As K/L, Bi L/M ratios from Monte Carlo simulations as function of GaAsBi thickness (acceleration voltage: 200 kV, take-off angle: 25°, density 5.36 g cm^{-3} for $x = 0.2$).

function of a heavy element's K/L ratio instead of absolute specimen thickness, this reduces both the dependence on real foil thickness measurements[14] and the effect of detector sensitivities changing with detector type or entrance window thickness.[15] The reason for this is that a change in the detector sensitivity curve will change the K/L ratios measured and thereby give another value on the same set of calibration curves for k*, providing an inherent self-calibration against changes in detector sensitivities. We have previously shown how this method allowed as to measure highly accurately the germanium content in elemental semiconductors[16] or the indium content in compound semiconductors[17] and will extend this here to GaAsBi.

Using the standard notation (A for atomic densities, k_{AB} for sensitivity factor of line A versus line B of another element and I_A for intensity from line A), there are three different ways to measure the bismuth content x of an alloy $Ga(As_{1-x}Bi_x)$ where Bi substitutes for As, namely

2.1 | Measuring Bi relative to the fixed Ga content of the group III sub-lattice

$$x = \frac{I_{Bi} k^*_{Bi,Si}/A_{Bi}}{I_{Ga} k^*_{Ga,Si}/A_{Ga}} \tag{1}$$

from which we can determine the relative k*-factor as

$$k^*_{Bi,Ga} = x \frac{A_{Bi}}{A_{Ga}} \frac{I_{Ga}}{I_{Bi}}, \tag{2}$$

where we could use sets of four different k*-factors $k^*_{BiX,GaY}$ for two Bi X-ray lines (X = L or M) and two Ga X-ray lines (Y = K or L).

2.2 | Measuring Bi relative to the As content (1–x) within the group V sub-lattice

$$x = \frac{I_{Bi} k^*_{Bi,Si}/A_{Bi}}{I_{As} k^*_{As,Si}/A_{As} + I_{Bi} k^*_{Bi,Si}/A_{Bi}} = \frac{I_{Bi} k^*_{Bi,As} A_{As}}{I_{As} A_{Bi} + I_{Bi} k^*_{Bi,As} A_{As}} \tag{3}$$

from which we can determine the relative k*-factor as

$$k^*_{Bi,As} = \frac{x}{1-x} \frac{A_{Bi}}{A_{As}} \frac{I_{As}}{I_{Bi}} \tag{4}$$

and again can use four different sets $k^*_{BiX,AsY}$ for two Bi X-ray lines (X = L or M) and two As X-ray lines (Y = K or L).

2.3 | Measuring the Bi content relative to all other elements, Ga and As

$$x = 2 \frac{I_{Bi} k^*_{Bi,Si}/A_{Bi}}{I_{Ga} k^*_{Ga,Si}/A_{Ga} + I_{As} k^*_{As,Si}/A_{As} + I_{Bi} k^*_{Bi,Si}/A_{Bi}}. \tag{5}$$

Note the atomic concentration of Bi in $Ga(As_{1-x}Bi_x)$ is $x/2$, hence the factor 2 in the above equation. Multiplication of both numerator and denominator by

$k^*_{Si,As} A_{Ga} A_{As} A_{Bi}$ and considering transitivity

$$k_{AB}\, k_{BC} = k_{AC} \tag{6}$$

as well as inversion

$$k_{AB} = 1/k_{BA} \tag{7}$$

gives

$$x = 2\frac{I_{Bi} k^*_{Bi,As} A_{Ga} A_{As}}{I_{Ga} k^*_{Ga,As} A_{As} A_{Bi} + I_{As} A_{Ga} A_{Bi} + I_{Bi} k^*_{Bi,As} A_{Ga} A_{As}} \tag{8}$$

wherein

$$k^*_{Ga,As} = \frac{1}{1-x}\,\frac{A_{Ga}}{A_{As}}\,\frac{I_{As}}{I_{Ga}} \tag{9}$$

describes again four different sets $k^*_{GaX,AsY}$ for two Ga X-ray lines (X = K or L) and two As X-ray lines (Y = K or L) that can be taken from stoichiometric GaAs.

In summary, there are a dozen dimensionless k^*-factors that can be used to determine x in different ways, as given by Equations (2), (4) and (9), four each relative to Ga (i) or to As (ii) as in binary alloys and also four for Ga and As (iii) in the ternary alloy. Most software programs for X-ray analysis try to fit and use all elements available, as in option (iii) but then choose only one of the four possible sets of line combinations and often do not give the user a choice. A user would thus typically get one numerical result but have no idea what the expected error would be.

If a user has an experimental spectrum of $GaAs_{1-x}Bi_x$, they can determine k^*-factors for the measured line intensities $I_{Ga,\,As,\,Bi}$ and nominal x values using Equations (2), (4) and (9) as described here and then use these to calculate new x-values from Equations (1), (3) and (8), respectively, which should all lie much closer together than any standard quantification routine would allow.

3 | EXPERIMENT

Growth details, photoluminescence (PL) and X-ray diffraction (XRD) results of the GaAsBi sample studied here (sample ID number STB 29) have been described earlier in Ref. (18). The sample contains a thin and a thicker $GaAs_{1-x}Bi_x$ quantum well (QW) grown at 320°C with GaAs barriers, where PL and XRD indicated $x \approx 0.112$ but STEM-EDX showed only the thicker quantum well reached a constant Bi content.[19] In the following, quantification of a series of several X-ray spectra taken in the centre of the 17 nm thick $Ga(As_{1-x}Bi_x)$ quantum well (cf. Figure 6A) is performed by comparing results from all 12 possible combinations of k^*-factors as outlined above. Figure 2 shows the sum spectrum. For a GaAs sample thinner than 100 nm the total electron beam spread at the underside of the sample (diameter with 90% of the signal) would be less than 10 nm for 200 keV electrons, so the X-ray signal from the 17 nm wide GaAsBi quantum well studied edge-on will stem from the quantum well only, ensuring we are really sampling the GaAsBi layer without including its surrounding matrix.

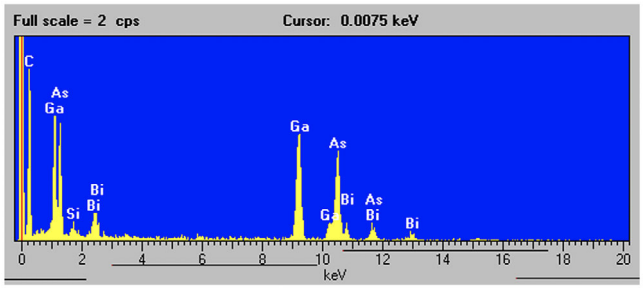

FIGURE 2 Energy-dispersive X-ray spectrum (EDXS) from the centre of 17 nm thick layer of GaAsBi in the JEOL 2010F. Acquisition details: 197 kV acceleration voltage, 25° take-off angle, Si:Li with ultrathin Moxtek window, 20 eV channel^{-1} dispersion, 743 s total acquisition time, 3.7% deadtime. Sample thickness is estimated by ISIS to lie around 80 nm.[18]

Quantification of the Bi and Ga X-ray lines using the in-built Oxford Instruments ISIS 300 software on a JEOL 2010F, with absorption correction, yielded apparent Bi concentrations that depended strongly on the X-ray lines chosen, from 7.7% ± 0.7% for Bi_M/Ga_K, over 10.7% ± 1.8% for Bi_L/Ga_L to 14.6% ± 1.7% for Bi_M/Ga_L.[18] Their average of $x_{ISIS,2lines} = 0.110 \pm 0.035$ appeared to be in line with PL and is credible but the spread given by the standard deviation is too large to be really useful. Taking into account X-ray lines from all three elements apparently improved the situation a little, giving slightly lower values ranging from 7.3% ± 1.9% for Bi_M, Ga_K, As_K to 13.8% ± 2.2% for Bi_L, Ga_L, As_L, with less scatter around an average of $x_{ISIS,3lines}$ 0.103 ± 0.014.[19]

Most users would have stopped analysis here but it is shown in the following that simply averaging over different quantification options, some of which yield values that spread much more than deviations expected from counting statistics would suggest, will provide unreliable data, and a re-consideration of k^*-factors and sum peak overlaps using a self-consistent approach provides not only a much reduced spread but also shifts the apparent Bi content to larger values than expected. This has then been used to help understand statistics in atomically resolved high-resolution annular dark field (ADF) STEM images that we previously had difficulty to explain.

The original K/L ratios for Ga and As lines measured suggest specimen thicknesses around 260 nm (Ga K/L)

TABLE 2 Intensities summed over five experimental X-ray spectra shown in Figure 2 taken from the centre of the $Ga(As_{1-x}Bi_x)$ quantum well (JEOL 2010F, 200 kV, 25° ToA, Oxford Si:Li) and calculated ratios, originally without any correction.

Line	Intensity [counts]	K/L ratio	L/M ratio	Extrapolated foil thickness *t* [nm] from Figure 1
Ga K	7512 ± 177	1.804 ± 0.063 [1.577 ± 0.060]	–	260 ± 27 [161 ± 27]
Ga L	4164 ± 107			
As K	5670 ± 178	1.489 ± 0.061 [1.286 ± 0.058]	–	116 ± 18 [55 ± 18]
As L	3808 ± 101			
Bi L	1078 ± 95	–	0.665 ± 0.072 [1.055 ± 0.107]	−265 ± 85 [174 ± 116]
Bi M	1622 ± 103			

Note: Values in brackets with a correction for 600 sum peak counts at 2.4 keV to be transferred from Bi_M to each of Ga_L and As_L.

TABLE 3 Numerical results for $Ga(As_{0.89}Bi_{0.11})$ quantum well.

Lines	Equations used	*k**-factor used	*k* from ISIS for *t* = 0	*k** from CASINO for *t* = 1–8 nm	Value of *k** selected from best K/L fit	*x* from *k** without sum peak correct-ion for Bi_M	*x* from *k** with sum peak correct-ion for Bi_M
Bi, Ga	1, 2	Bi_M, Ga_L	1.047	2.10 ± 0.01	1.917 ± 0.079	0.249 ± 0.020	0.137 ± 0.020
		Bi_M, Ga_K	1.076	2.59 ± 0.08	3.351 ± 0.081	0.241 ± 0.017	0.152 ± 0.017
		Bi_L, Ga_L	1.782	2.34 ± 0.09	1.621 ± 0.036	0.140 ± 0.013	
		Bi_L, Ga_K	1.832	2.88 ± 0.02	2.901 ± 0.006	0.139 ± 0.013	
Bi, As	3, 4	Bi_M, As_L	1.054	2.06 ± 0.12	1.725 ± 0.034	0.208 ± 0.015	0.125 ± 0.015
		Bi_M, As_K	0.944	2.25 ± 0.07	2.536 ± 0.030	0.206 ± 0.015	0.141 ± 0.015
		Bi_L, As_L	1.794	2.24 ± 0.08	1.677 ± 0.077	0.145 ± 0.015	
		Bi_L, As_K	1.607	2.50 ± 0.12	2.490 ± 0.001	0.145 ± 0.014	
Ga, As	8, 9	Ga_L, As_L	1.007	0.964 ± 0.012	1.248 ± 0.048	0.128 ± 0.022	
		Ga_L, As_K	0.902	1.083 ± 0.005	1.356 ± 0.052	0.142 ± 0.015	
		Ga_K, As_L	0.979	0.772 ± 0.012	0.513 ± 0.029	0.159 ± 0.024	
		Ga_K, As_K	0.877	0.869 ± 0.005	0.857 ± 0.001	0.142 ± 0.013	

Note: Green [orange] values: Relative rms spreads of up to 1% [2%]. Red values: Data without sum peak correction. Error bars in Table 3 have been obtained from propagating standard errors in *k** from plots in Figures 3–5 and Equations (2), (4) and (9) from the statistical uncertainties in the measured line intensities I_x as given by $2/\sqrt{I_x}$ for each line where the factor 2 accounts for errors in background subtraction that are assumed to be of the same size as counting statistics. That is the reason error bars are larger if *k** plots have a larger slope or X-ray lines with low count numbers are involved.

or 120 nm (As K/L), respectively, but the Bi L/M ratio measured is much lower than what Monte Carlo simulations would suggest for any thickness, and a fit would only be obtained for a negative specimen thickness, which is unphysical. This indicates three issues:

(i) The As line intensities are much lower than the Ga line intensities, which can be simply explained by some Bi replacing As.
(ii) The As K/L line ratio is also much lower than the Ga K/L line ratio, which could be explained by secondary fluorescence from As L onto Ga L lines not taken account in the simulations.
(iii) The Bi M line intensity is much higher in intensity than expected, which could be due to some Ga and As L X-rays creating sum peaks (as indicated in Table 1), or the predicted *k*-factor for the Bi M-line relative to all other lines *X* being completely wrong.

We notice in Table 3 that ISIS predicts values of $k_{BiM,X}$ less than half of what Casino would predict for thin foils. For ~100 nm foil thickness, the latter would predict Bi L/M ratios around unity, that is, 50% larger than the value of 0.665 actually measured. This has tentatively been modelled assuming a certain number of counts, approximately 600 as found by iterative trial and error, of Ga L and As L lines, corresponding to about 15% of their line intensities, have been recorded simultaneously and their sum misinterpreted as due to Bi M. This correction would bring the experimentally measured Bi L/M ratio into the range predicted by Monte Carlo simulations in Figure 1. The values in brackets in Table 2 show how such a sum peak cor-

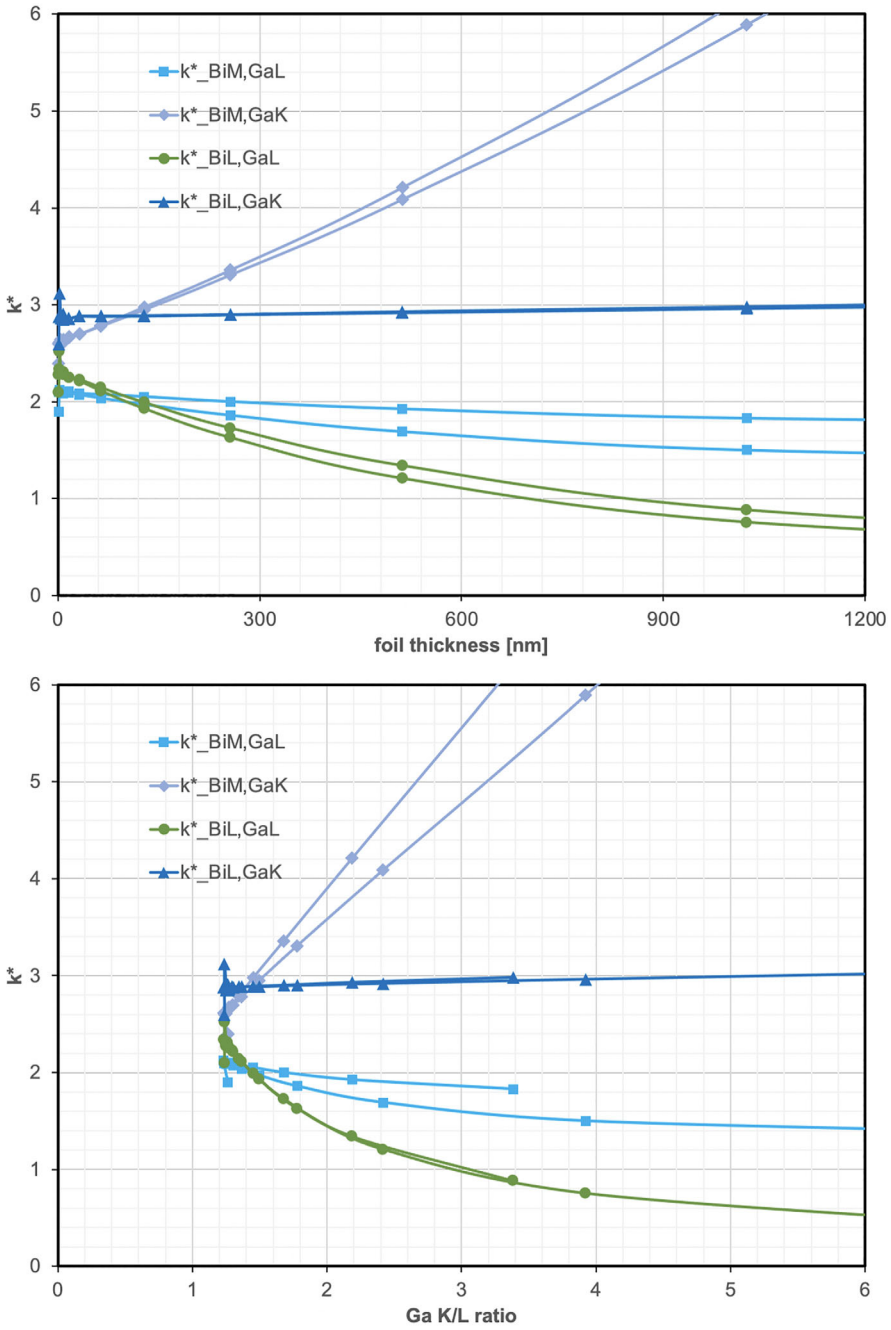

FIGURE 3 Plot of k^* factors of Bi lines with respect to Ga lines, either as function of thickness (top) or as function of Ga K/L ratio (bottom), for two alloys of different densities (5.34 g cm^{-3} for $x = 0.1$ and 5.36 g cm^{-3} for $x = 0.2$). All are exponential curves, where the ones for the lower x-value are slightly less curved and run both shorter and higher. The value of $k^*_{\mathrm{BiL,GaK}} \approx 2.895 \pm 0.034$ is almost constant for thicknesses up to 1 µm as both X-ray lines are of similar energy, so the selection of this line pair would seem particular useful for quantification.

rection brings K/L and L/M ratios and correspondingly extrapolated foil thicknesses into more realistic ranges, although the agreement from the three line ratios is still not perfect. While the uncertainty in absolute values of specimen thicknesses extrapolated from the three K/L and L/M ratios in Table 2 has been reduced from originally 37 ± 271 nm down to 130 ± 65 nm, this discrepancy is still rather large and could be reduced by further iteration; however, for the purpose of improving the absorption correction in EDXS this has been sufficient and further refinement was not performed.

Quantification without sum peak correction yields an apparent mean Bi content of $x_{\mathrm{app}} = 0.170 \pm 0.043$, which would be much higher than the quantification of $x_{\mathrm{ISIS}} =$

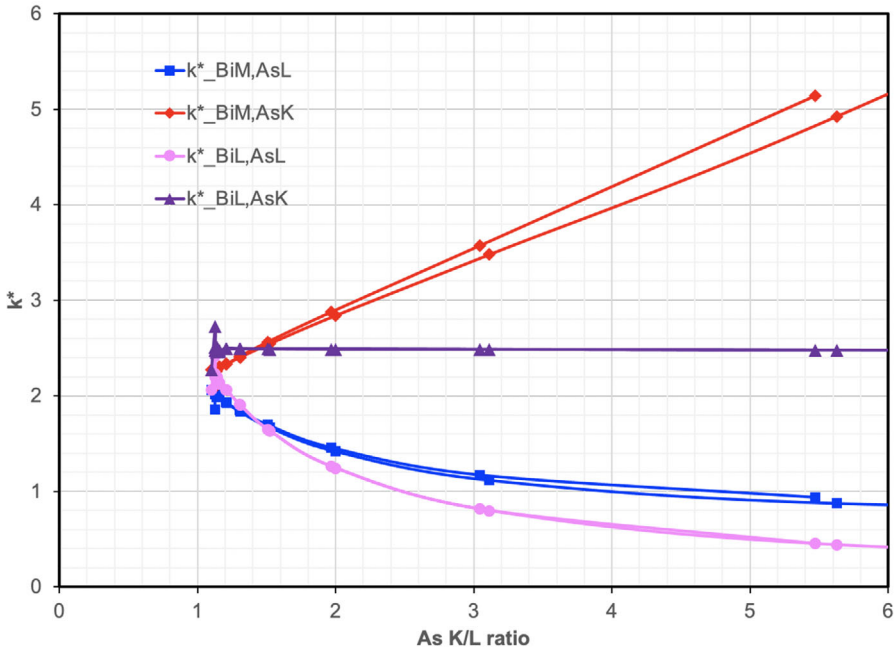

FIGURE 4 Plot of k^* factors of Bi lines with respect to As lines as function of As K/L ratio for two alloys of different densities (5.34 g cm^{-3} for $x = 0.1$ and 5.36 g cm^{-3} for $x = 0.2$). All are exponential curves, where the ones for the lower x-value are slightly less curved and run both shorter and higher. The value of $k^*_{\mathrm{BiL,AsK}} \approx 2.490 \pm 0.071$ is almost constant for thicknesses up to 1 μm as both X-ray lines are of very similar energy, so the selection of this line pair would also seem well suited for quantification.

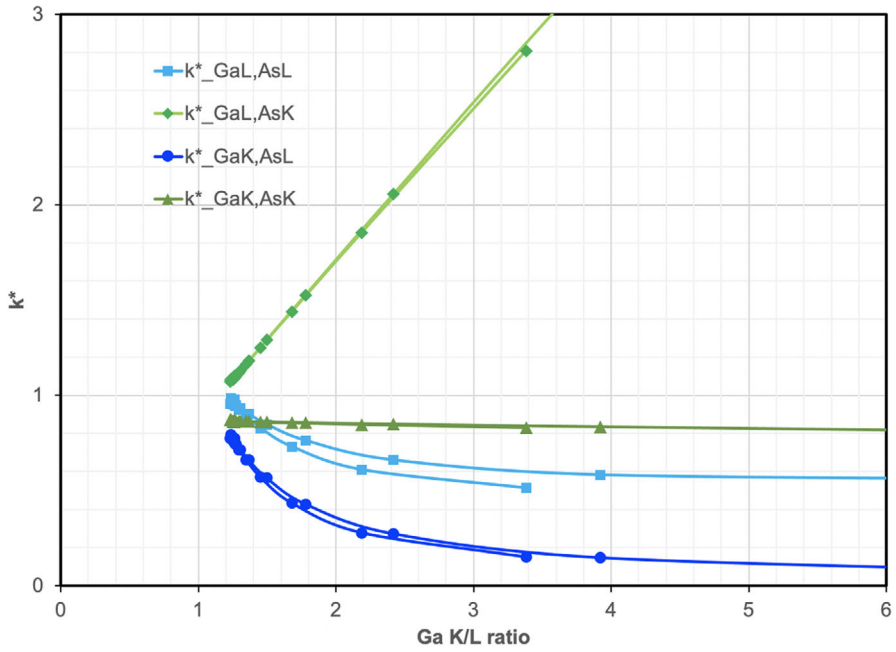

FIGURE 5 Plot of k^* factors of Ga lines with respect to As lines as function of Ga K/L ratio for two alloys of different densities (5.34 g cm^{-3} for $x = 0.1$ and 5.36 g cm^{-3} for $x = 0.2$). All are exponential curves, where the ones for the lower x-value are slightly less curved and run both shorter and lower. Note the expanded vertical scale. The value of $k^*_{\mathrm{GaK,AsK}} \approx 0.861 \pm 0.011$ is constant for thicknesses up to 1 μm as both X-ray lines are of similar energy, so the selection of this line pair would also seem good for quantification if the decrease in As signal could be as reliably measured as the direct increase in the Bi signal.

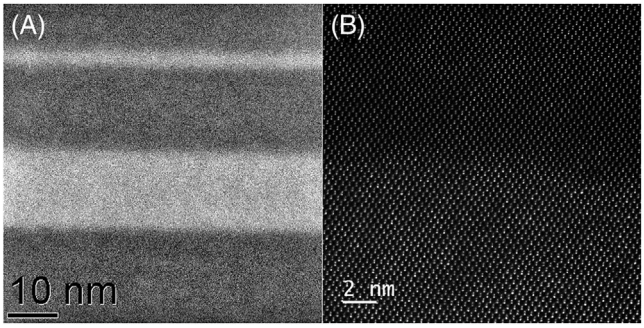

FIGURE 6 ADF STEM sample STB29. (A) Both quantum wells (QWs) imaged in JEOL 2010F, 197 keV, 0.25 nm electron beam, semi-angle of convergence: $\alpha = 9.5$ mrad, collection angle: $\beta \approx$ 50–170 mrad. (B) Upper GaAs-on-GaAsBi interface of wider QW imaged in JEOL ARM300CF, 300 kV, 0.1 nm electron probe, $\alpha =$ 19 mrad, $\beta \approx$ 48–221 mrad.

0.110 ± 0.035 and show an even larger spread. In fact, such large x values would lie outside the physical range of possible Bi contents at the rather low growth temperature used.[20] If the sum peak problem is resolved, however, then the quantification from all 12 k^* values in Table 3 gives $x_{k^*} = 0.141 \pm 0.009$ where their rms spread is even smaller (± 0.008) if the different values are weighted with factors corresponding to the inverse of their variances. A detection limit would be typically set at 3 times that standard deviation, that is, ± 0.025, which is not that low because it is ultimately limited by the relative low count numbers here, of the order a few thousands, due to the fact we tried to keep the electron beam near the centre of the quantum well. Had sensitivity been a question we should have collected many more counts to reduce that noise floor further, at the risk of getting more drift. The accuracy represented by the standard error of the mean would be the above standard deviation divided by the square root of the number N of independent measurements (here: $N = 6$ X-ray lines), giving ± 0.004 and thus approach best detection limits (!) in EDXS. The value of $x_{k^*} = 0.141 \pm 0.009$ lies at the upper limit of possible bismuth content physically possible at 320°C[20] and at the same time gives a much better agreement with Binomial statistics appropriate for a random alloy[21,22] when we analyse the intensity fluctuations of high-angle ADF STEM images from very thin samples, as shown in Figures 6B and 7. From Ref. (23), we can extrapolate the exponent with which the intensity in Figure 6B follows the atomic number contrast as $\varepsilon = 1.9$, so a Bi atom should be about 5.8× brighter than an As atom, which is necessary to evaluate the image contrast in Figure 7. GaAs from the area above the QW (without any significant number of Bi atoms) shows a broad intensity distribution that can be well fitted by a Poisson distribution ($\lambda = 4$, peak at: 3838 ± 171) while GaAsBi from the QW shows a much wider Binomial distribution (mean: 4534 ± 383) with faint discrete peaks. The specimen thickness is around 10 nm, corresponding to $N = 25$ atoms. The peaks indicated by the open squares are about 190 intensity units apart and correspond to $M = 0, 1, 2, \ldots, 10$ individual Bi atoms within the atomic columns. The highest peaks at $M = 3$ and $M = 4$ are about equal in height, confirming an average Bi content of $3.5/25 = 0.14 = x$ and could not have been explained with much lower x-values.

The key point in this study was to realise that measured Bi L/M ratios seemed to contradict values from Monte Carlo simulations for all thicknesses. The ISIS software for automated quantification either ignored the Bi M line by choosing the Bi L line as default instead or, if forced, 'fudged' quantification using the Bi M-line by assigning it an artificially low k-factor, however, this could not solve the problem of large spread in compositional quantification for other X-ray lines. A manual identification of the sum peak at 2.4 keV and a corresponding count re-distribution were necessary until all measured K/L and L/M ratios gave reasonable first thickness estimates. Finally, k^* factor quantification using the product of thin film k-factors and absorption correction factors most appropriate for the observed K/L ratios of the more abundant elements (Ga and As) and the M/L ratio of the least abundant (Bi) gave self-consistent values with a root mean-squared (rms) error of $\Delta x < 1$ % that was finally limited by counting statistics. The average concentration of the 17 nm $GaAs_{1-x}Bi_x$ quantum well was determined as $x = 0.141$ with an expected mean error of ± 0.003, which lies at the higher end of what most standard routine quantification options yielded here and at the same time represents the maximum Bi content obtainable in such alloys by molecular beam epitaxy at 320°C according to the scatter plot shown in Figure 7 of Ref. (20).

4 | CONCLUSION

Quantitative analyses of the Bi content of GaAsBi alloys from STEM-EDX that use standard k-factors and absorption correction procedures but without explicit sum peak consideration for the Bi M-line (as in Refs. 22, 24–26) should be re-evaluated carefully in the light of the present results as they will likely underestimate the Bi content significantly, by about 37% relative, which can already amount to more than 1 at% error if apparently $x \approx 0.03$ while $x = 0.04$ in reality. Compiling tables of line ratios from which foil thicknesses can be estimated (Table 2) and calculated k^*-factors that can be used for compositional evaluations from elemental X-ray line pairs (Table 3) is, for a given materials system, possible manually, as shown here, but tedious. A more computationally efficient

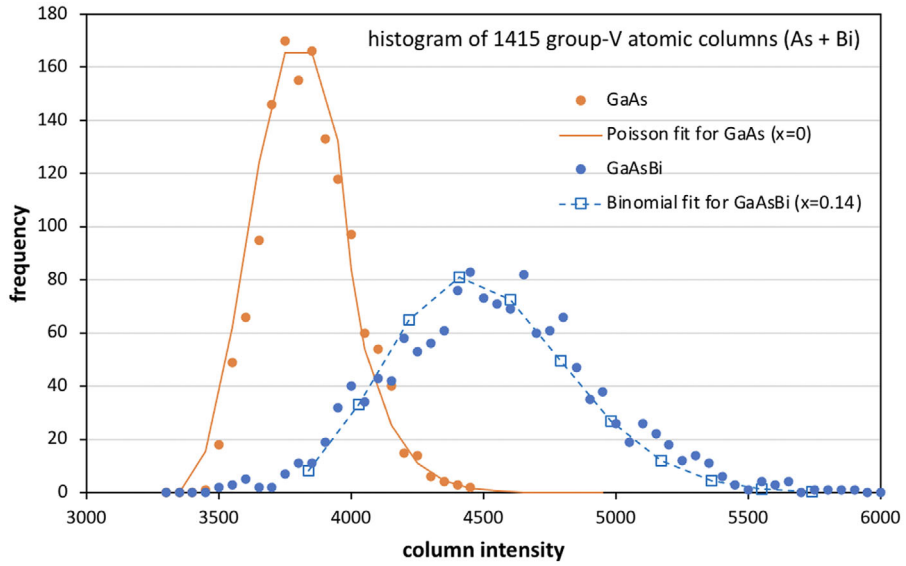

FIGURE 7 Statistical analysis of the intensities of the lower group V columns (As, Bi) in Figure 6B.

semi-automated approach would, after identification of X-ray lines and all sum and escape peaks, employ K/L and/or L/M ratio measurements for the heavier elements to automatically estimate and update projected foil thicknesses iteratively. Then corresponding absorption correction factors could be calculated automatically for all lines from Monte Carlo simulations, and consistency be checked by using all X-ray line pairs for quantification rather than just one for a specific sub-set as is presently the default in most quantification programs.

For Ga(As,Bi), this approach is shown here to yield a dozen highly consistent values of the bismuth content, with errors below ±0.01 for Bi content as high as $x = 0.14$, and corresponding smaller systematic errors for lower Bi content. The author does not see a risk of model overfitting here because the only assumptions made are that the product of thin film *k*-factors and absorption correction factors (exponentials given by Lambert-Beer's law) used to convert experimental X-ray intensities into concentrations should yield, for a given spectrum, the same results within statistical errors, independent of which X-ray lines are actually used for quantification. The predictive power of this *k** factor approach has so far been successfully tested for several SiGe and InGaN alloys; the only addition to the GaAsBi system considered here has been to take into account possible Ga and As L sum peaks contributing to the apparent Bi M line intensity. It is perhaps interesting to note in this context that while the latter correction has reduced the corrected Bi M line intensity and so the apparent value of Bi content determined from this line, the overall result has been a convergence of compositional values thus determined towards the upper limit of the range of values obtained using previous quantification routines. For the future, it is planned to test this quantification procedure also for thicker GaAsBi layers of lower bismuth content.

ACKNOWLEDGEMENTS

The author wishes to thank E. Liberti for operating the ARM300CF (instrument E02) of the electron Physical Science Imaging Centre (ePSIC) at Diamond Light Source, Harwell, UK. Access was provided by grant EM16985 'Single Bi atom mapping in thin GaAsBi quantum well specimen'.

ORCID

T. Walther https://orcid.org/0000-0003-3571-6263

References

1. Panek, M., Ratuszek, M., & Tlaczala, T. (1986). LPE grown GaAs layers from Ga–As–Bi solution. *Journal of Crystal Growth*, *74*, 568–574.
2. Tixier, S., Adamcyk, M., Tiedje, T., Francoeur, S., Mascarenhas, A., Wei, P., & Schiettekatte, F. (2003). Molecular beam epitaxy growth of $GaAs_{1-x}Bi_x$. *Applied Physics Letters*, *82*, 2245–2247.
3. Yoshimoto, M., Murata, S., Chayahara, A., Horino, Y., Saraie, J., & Oe, K. (2003). Metastable GaAsBi alloy grown by molecular beam epitaxy. *Japanese Journal of Applied Physics*, *42*, L1235–L1237.
4. Lewis, R. B., Masnadi-Shirazi, M., & Tiedje, T. (2012). Growth of high Bi concentration $GaAs_{1-x}Bi_x$ by molecular beam epitaxy. *Applied Physics Letters*, *101*, 082112.
5. Balades, N., Sales, D. L., Herrera, M., Tan, C. H., Liu, Y., Richards, R. D., & Molina, S. I. (2018). Analysis of Bi distribution in epitaxial GaAsBi by aberration-corrected HAADF-STEM. *Nanoscale Research Letters*, *13*, 125.

6. Madouri, D., Boukra, A., Zaoui, A., & Ferhat, M. (2008). Bismuth alloying in GaAs: A first principles study. *Computational materials science*, *43*(4), 818–822.
7. X-ray transition energies database from the National Institute of Standards and Technology, USA. https://physics.nist.gov/PhysRefData/XrayTrans/Html/search.html
8. Table 1-2 of the X-ray Data Booklet from the Lawrence Berkeley National Lab, USA. https://xdb.lbl.gov/Section1/Table_1-2.pdf
9. Walther, T. (2010). Comparison of experimental and theoretical X-ray intensities from (In)GaAs specimens investigated by energy-dispersive X-ray spectroscopy in a transmission electron microscope. *Journal of Physics: Conference Series*, *209*, 012029.
10. Walther, T. (2010). An improved approach to quantitative X-ray microanalysis in (S)TEM: Thickness dependent *k*-factors. *Journal of Physics: Conference Series*, *241*, 012016.
11. Parri, M. C., & Walther, T. (2012). Determining sample thickness in transmission electron microscopy using X-ray line intensity ratios. In *15th European Microscopy Congress, Vol. 2(Physical Sciences: Tools and Techniques) (pp 645-646)*, Vol. 2 (pp. 645–646). Oxford.
12. Hovington, P., Drouin, D., & Gauvin, R. (1997). CASINO: A new Monte Carlo code in C language for electron beam interaction—Part I: Description of the program. *Scanning*, *19*(1), 1–14.
13. Cliff, G., & Lorimer, G. W. (1997). Quantitative analysis of thin specimens. *Journal of Microscopy*, *103*, 203–207.
14. Walther, T., & Wang, X. (2015). Self-consistent absorption correction for quantitative energy-dispersive X-ray spectroscopy of InGaN layers in analytical electron microscopy. *Journal of Physics: Conference Series*, *644*, 012006.
15. Parri, M. C., Qiu, Y., & Walther, T. (2015). New pathways for improved quantification of energy-dispersive X-ray spectra of elements with multiple X-ray lines from thin foils investigated in transmission electron microscopy. *Journal of Microscopy*, *260*(3), 427–441.
16. Qiu, Y., Nguyen, V. H., Dobbie, A., Myronov, M., & Walther, T. (2013). Calibration of thickness-dependent k-factors for germanium X-ray lines to improve energy-dispersive X-ray spectroscopy of SiGe layers in analytical transmission electron microscopy. *Journal of Physics: Conference Series*, *471*, 012031.
17. Walther, T., & Wang, X. (2016). Self-consistent method for quantifying indium content from X-ray spectra of thick compound semiconductor specimens in a transmission electron microscope. *Journal of Microscopy*, *252*(2), 151–156.
18. Bastiman, F., Qiu, Y., & Walther, T. (2011). GaAsBi atomic surface order and interfacial roughness observed by STM and TEM. *Journal of Physics: Conference Series*, *326*, 012060.
19. Walther, T., Richards, R. D., & Bastiman, F. (2015). Scanning transmission electron microscopy measurement of bismuth segregation in thin Ga(As,Bi) layers grown by molecular beam epitaxy. *Crystal Research and Technology*, *50*(1), 38–42.
20. Richards, R. D., Bailey, N. J., Liu, Y., Rockett, T. B. O., & Mohmad, A. R. (2022). GaAsBi: From molecular beam epitaxy growth to devices. *Physica Status Solidi*, *259*, 2100330.
21. Walther, T., Humphreys, C. J., Grimshaw, M. P., & Churchill, A. C. (1995). Detection of random alloy fluctuations in high-resolution transmission electron micrographs of AlGaAs. *Philosophical Magazine A*, *71*(4), 1015–1030.
22. Paulauskas, T., Pacebutas, V., Butkute, R., Cechavicius, B., Naujokaitis, A., Kamarauskas, M., Skapas, M., Devenson, J., Caplovicova, M., Vretenar, V., Li, X., Kociak, M., & Krotkus, A. (2020). Atomic-resolution EDX, HAADF, and EELS study of $GaAs_{1-x}BI_x$ alloys. *Nanoscale Research Letters*, *15*, 121.
23. Walther, T. (2006). A new experimental procedure to quantify annular dark field images in scanning transmission electron microscopy. *Journal of Microscopy*, *221*(2), 137–144.
24. Braza, V., Fernandez, D., Ben, T., Flores, S., Bailey, N. J., Carr, M., Richards, R., & Gonzalez, D. (2024). Exploring the implementation of GaAsBi alloys as strain-reducing layers in InAs /GaAs quantum dots. *Nanomaterials*, *14*, 375.
25. Braza, V., Ben, T., Reyes, D. F., Bailey, N. J., Carr, M. R., Richards, R. D., & Gonzalez, D. (2025). Structural and optical characteristics of epitaxially grown AlGaAsBi on GaAs for potential application in ultra-low noise avalanche photodiodes. *Applied Surface Science*, *698*, 162473.
26. Flores, S., Reyes, D. F., Braza, V., Bailey, N. J., Carr, M. R., Richards, R. D., & Gonzalez, D. (2025). The effects of growth interruptions in the GaAsBi/InAs/GaAs quantum dots: The emergence of three-phase nanoparticles. *Surface & Interface*, *56*, 105490.

How to cite this article: Walther, T. (2025). Determining bismuth content in GaAsBi alloys by energy-dispersive X-ray spectroscopy: A case study with multiple sets of *k**-factors for analytical transmission electron microscopy. *Journal of Microscopy*, 1–10. https://doi.org/10.1111/jmi.70058